GMAW 系统电流与弧长的滑模变结构控制仿真

高忠林[1], 胡绳荪[1], 殷凤良[1], 王 睿[2]
(1. 天津大学 材料科学与工程学院, 天津 300072;
2. 河北工业大学 电气与自动化学院, 天津 300130)

高忠林

摘 要: 在分析熔化极气体保护焊(GMAW)的基础上, 建立电流及弧长的非线性数学模型。应用基于微分几何的反馈线性化方法, 将 GMAW 过程电流及弧长模型同胚映射为等价的线性系统, 使复杂的非线性控制问题转化成简单的线性系统的控制问题, 使控制器设计的复杂程度降低, 控制效果明显优于对非线性系统的直接控制。把滑模变结构控制方法应用于焊接电流及弧长的控制中, Matlab 仿真结果表明, 该方法可以满足焊接中电弧弧长的精确控制, 同时, 对系统参数摄动和外部扰动具有较强的鲁棒性。

关键词: 熔化极气体保护焊; 滑模变结构控制; 反馈线性化; 鲁棒性
中图分类号: TG431.5 文献标识码: A 文章编号: 0253－360X(2007)06－053－04

0 序 言

熔化极气体保护焊(gas metal arc welding, GMAW)作为一种高效的焊接方法, 广泛应用于手工及机器人自动焊接生产线。为了提高 GMAW 焊接质量, 国内外学者对 GMAW 焊接过程的控制进行了大量的研究, 提出了许多行之有效的控制方法。这其中有弧长反馈闭环控制法, 自适应闭环控制以及门限控制法等[1]。这些控制方法的缺点是其鲁棒性较差, 焊接过程稳定性欠佳。鉴于此, 应用滑模变结构控制来实现 GMAW 系统弧长的控制。

滑模变结构控制是变结构控制系统的一种控制策略。这种控制策略与常规控制的根本区别在于控制的不连续性, 即一种使系统"结构"随时间变化的开关特性。该控制特性可以迫使系统在一定条件下沿规定的状态轨迹作小幅度、高频率的上下运动, 即滑动模态。系统在这种滑动运动模态下, 对系统干扰及参数变化具有完全的自适应性或不变性。这样, 处于滑模运动的系统就具有很好的鲁棒性。而这种鲁棒性正是实现高质量焊接控制所要求的。

1 GMAW 过程数学模型

GMAW 过程如图 1 所示, 焊接过程中, 电弧从焊接电源获得能量, 来保证其自身的燃烧。在这其中, 不断熔化焊丝并将其过渡到焊件上去, 从而达到焊接的目的。为了提高焊接质量, 必须对电弧电压和焊接电流加以控制。通常所采用的方法是反馈控制, 其原理如图 2 所示。

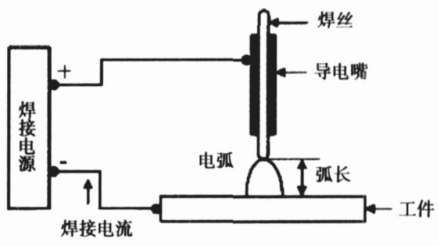

图 1 GMAW 系统示意图
Fig. 1 Illustration of GMAW

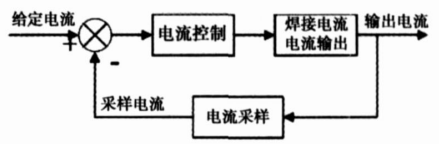

图 2 焊接电流控制原理图
Fig. 2 Schematic arawing of current closed－loop control of GMAW

设输出电流(实际焊接电流)为 I, 给定电流为 I_g, 由图 2 可知, 其电流的传递函数可用一阶系统来表示, 即

$$I = \frac{1}{s\tau + 1} I_g, \tag{1}$$

式中: τ 为时间常数; s 为复数。对上式进行拉普拉斯反变换, 得式(2)为

收稿日期: 2006－07－10
基金项目: 天津市自然科学基金资助项目(05YFJMJC08900)

$$\dot{I} = -\frac{1}{\tau}I + \frac{1}{\tau}I_g。 \tag{2}$$

在GMAW过程中，电弧长度 l_{arc} 是送丝速度 v_e、焊丝熔化速度 v_m 以及导电嘴到工件的距离 l_{CT} 的函数[2,3]。电弧长度的变化为

$$\frac{\mathrm{d}l_{arc}}{\mathrm{d}t} = v_m - v_e。 \tag{3}$$

根据文献[4]，焊丝熔化速度模型如式(4)所示。将式(4)代入式(3)，得电弧长度的变化如式(5)所示。

$$v_m = k_1 I + k_2 I^2 (l_{CT} - l_{arc}), \tag{4}$$

$$\frac{\mathrm{d}l_{arc}}{\mathrm{d}t} = k_1 I + k_2 I^2 (l_{CT} - l_{arc}) - v_e。 \tag{5}$$

将式(2)和式(5)写成状态空间表达式得到式(6)，即

$$\begin{cases} \dot{x} = f(x) + g(x)u, \\ y = h(x)。 \end{cases} \tag{6}$$

式中：$f(x) = \begin{bmatrix} -\frac{1}{\tau}x_1 \\ k_1 x_1 + k_2 x_1^2 (l_{CT} - x_2) - v_e \end{bmatrix}$；

$g(x) = \begin{bmatrix} \frac{1}{\tau} \\ 0 \end{bmatrix}$；$h(x) = x_2$；$x$ 为二维状态变量；$x_1 = I$；$x_2 = l_{arc}$；u 为给定输入量，$u = I_g$；y 为输出函数，$y = l_{arc}$；k_1，k_2 为熔化速度常数。

由式(6)可以看出，其为一典型的单输入单输出仿射非线性控制系统。

2 反馈线性化

对于式(6)所示的非线性系统，通常按泰勒级数展开，取其线性部分，称为线性近似。为了提高控制精度，这里采用精确线性化(exact linearization)。这种方法相比于泰勒级数展开而言，其在线性化过程中没有忽略掉任何高阶非线性项，因此其不仅精确，而且是整体的，即线性化对变换有定义的整个区域都适用[5]。

对式(6)中 y 求导可得

$$\dot{y} = \frac{\partial h}{\partial x} f(x) + \frac{\partial h}{\partial x} h(x) u = L_f h(x) + L_g g(x) u, \tag{7}$$

式中：$L_f h(x)$，$L_g g(x)$ 分别代表 h 对向量场 f 和 g 的李导数(lie derivative)。如果 $L_g g(x)$ 不等于0，则通过状态反馈律式(8)可以得到输出 y 对新输入 v 的一阶线性系统如式(9)所示。

$$u = \frac{1}{L_g g(x)} [-L_f h(x) + v], \tag{8}$$

$$\dot{y} = v, \tag{9}$$

式中：v 为新的输入量。于是存在函数 $\alpha(x)$ 及 $\beta(x)$，使得当 $u = \alpha(x) + \beta(x)v$ 时，系统的输入/输出是呈线性对应关系的。如果 $L_g g(x)$ 等于0，则须对式(7)求高阶导数。其状态反馈为

$$u = \frac{1}{L_g L_f^{\gamma-1} h(x)} [-L_f^{\gamma} h(x) + v], \tag{10}$$

式中：γ 为相对阶。通过式(10)可以将输入输出简化为

$$y^{(\gamma)} = v。 \tag{11}$$

根据上述方法则有

$$u = \frac{v - L_f^2 h(x)}{L_g L_f h(x)}。 \tag{12}$$

利用式(11)和坐标变换有

$$z = \begin{pmatrix} z_1 \\ z_2 \end{pmatrix} = \begin{pmatrix} h(x) \\ L_f h(x) \end{pmatrix} \begin{pmatrix} x_2 \\ k_1 x_1 + k_2 x_1^2 (l_{CT} - x_2) - v_e \end{pmatrix}, \tag{13}$$

式中：$z_1 = l_{arc}$；$z_2 = \dot{l}_{arc}$。

3 基于反馈线性化的GMAW系统滑模控制器的设计

3.1 滑模控制简介

考虑一般情况下，在系统的状态空间中，有一个切换面 a，它将状态空间分成上下两部分 $a>0$ 及 $a<0$。在切换面上的运动点有三种情况，如图3所示。

通常点——系统运动点运动到切换面 $a=0$ 附近时，穿越此点而过(点A)。

起始点——系统运动点运动到切换面 $a=0$ 附近时，从切换面的两边离开该点(点B)。

终止点——系统运动点运动到切换面 $a=0$ 附近时，从切换面的两边趋向于该点(点C)。

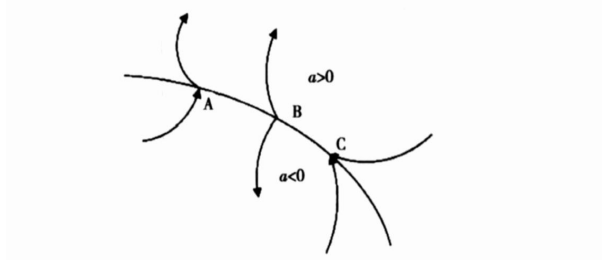

图3 切换面上三种点的特性

Fig. 3 Characteristic of three kind points on sliding surface

在滑模变结构中，通常点与起始点无多大意义，而终止点却有特殊的含义。因为如果在切换面上某一区域内所有的运动点都是终止点，则一旦运动点趋近于该区域，就会被“吸引”到该区域内运动。这对设计控制器具有极重要的意义[6]。

3.2　滑模变结构控制器的设计

经过反馈线性化后，焊接电流弧长非线性模型转化为单输入单输出线性系统，如式(13)所示。线性系统以 v 为输入，以 z_1 为输出。z_1 为电弧的长度。给定一定的电弧长度 l_g 后，就变为一个典型的跟踪问题。

定义偏差变量为

$$e = R - z = [e_1 \quad e_2]^T, R = [l_g, \dot{l}_g]^T, \quad (14)$$

式中：R 为期望输出；e 为偏差。

由于线性切换函数在滑动模态的稳定性与品质问题在线性系统理论中已得到解决，所以对于已经线性化的本系统，宜采用线性切换函数来简化系统的分析和设计。在此，选择切换面

$$a = ce_1 + e_2, \quad (15)$$

式中：c 为常数。在切换面上有 $a = 0$，故切换面上的滑模运动方程为

$$ce_1 + e_2 = 0。 \quad (16)$$

适当选取常数 c 的值，保证该动力学方程的稳定性和品质，便可保证滑模控制系统的存在性、可达性、稳定性这三个基本要求[7]。

上面设计出了切换面，但是这样的切换面未必是滑动面。要使切换面成为滑动面，关键是要设计变结构控制，使系统的任一初始状态能在变结构控制的作用下在有限时间到达切换面，此时切换面才是滑动面。系统状态一旦到达滑动面就不会离开，而是在上面滑动并趋向“原点”。在变结构控制理论中，状态点趋向滑动面的过程称为正常运动，在滑动面上的运动称为滑模运动。若切换函数为 a，则状态可达切换面的必要条件是 $a\dot{a} < 0$。此条件丝毫也反映不出运动是如何趋近切换面的，而正常运动的品质正是要求此趋近过程良好，比如快速。因此可以提出并发展趋近律的概念和公式，来保证正常运动的品质。可以设计出各种各样的趋近律[5]。

采用指数趋近率，指数趋近率的形式如下式所示

$$\dot{a} = -\varepsilon \mathrm{sgn}(a) - ka, k > 0, \varepsilon > 0, \quad (17)$$

式中：sgn 为符号函数；ε，k 分别为决定系统运动形式的待定系数，其选取原则是 ε 较小而 k 较大，这样既能加快正常运动的速度，又不至于使状态点“冲过”切换面而发生较大“抖动”。

根据式(14)，(15)及(16)，可解得滑模控制律为

$$u = \frac{-\varepsilon \mathrm{sgn}(a) - ka - ce_2 - L_f^2 h(x)}{L_g L_f h(x)}。 \quad (18)$$

4　仿真与分析

为了检验滑模变结构控制器的控制效果，对上述控制方法运用 Matlab 进行仿真。模型中的各参数的具体值以及单位如表 1 所示。仿真中设定弧长最后的稳定值为 3 mm，此时电流输出为 125 A 左右。图 4为滑模运动的相轨迹，由图中可以看出，当系统进入滑模状态后，将沿着切换面 a 运动，此时 $a=0$ 及 $\mathrm{d}a/\mathrm{d}t=0$。说明文中所设计的控制器，其滑动模态存在。图 5为弧长的收敛过程，从图中可以看出，其经过很短的时间(大约1 s左右)后就收敛在所设定的电弧长度3 mm上。图 6 和图 7 分别为滑模控制器的输出和电流仿真输出结果，从中可以看出其电流输出值与给定值相一致。

表 1　模型中各参数取值

Table 1　System parameters

参数	熔化速度常数 1 k_f/(m·s^{-1}·A^{-1})	熔化速度常数 2 k_2/(A^{-2}·m^{-1})	时间常数 τ/s	距离 l_{CT}/m	速度 v_d/(m·s^{-1})
数值	3.7×10^{-4}	6.6×10^{-4}	6.7×10^{-6}	0.015	0.267
意义描述	取决于焊丝电阻率、直径、伸出长度及电流数值	取决于弧柱电位梯度，弧长的数值	根据电路具体参数而得到	导电嘴到工件的距离	焊丝的送进速度

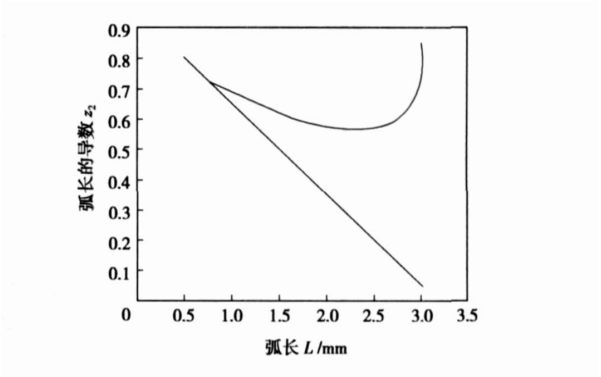

图 4　滑模运动的相轨迹

Fig. 4　Phase locus of sliding mode controller

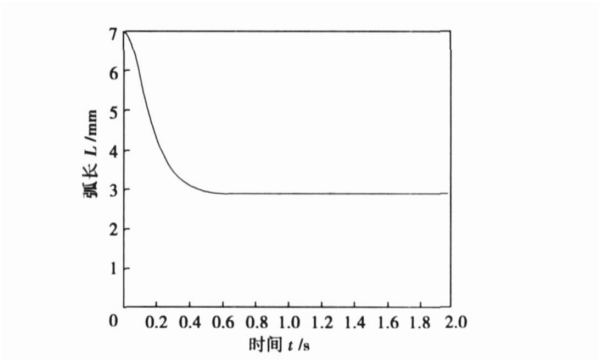

图 5　弧长的收敛过程

Fig. 5　Simulation output of arc length

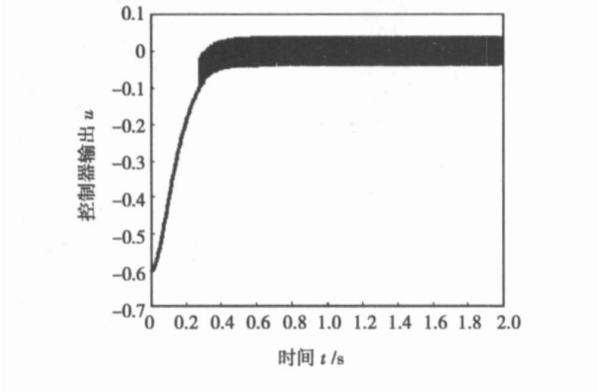

图 6 滑模控制器的输出

Fig. 6 Output of sliding mode controller

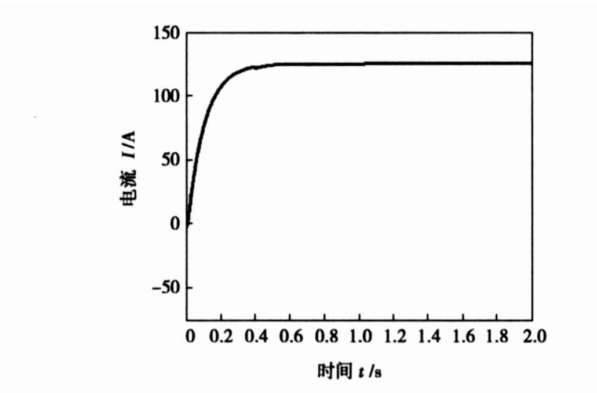

图 7 电流仿真输出结果

Fig. 7 Simulation output of current

5 结 论

(1) 根据非线性控制理论, 将GMAW 过程电流及弧长模型同胚映射为等价的线性系统, 使复杂的非线性控制问题转化成简单的线性系统的控制问题。

(2) 根据滑模控制原理, 将此种控制方法应用到电弧弧长的控制中, 使系统具有更强的抗干扰能力。

(3) 运用 Matlab 仿真表明, 滑模控制方法可以满足焊接中电弧弧长的精确控制。

参考文献:

[1] Pan Jiluan, Qu Zhiming, Wu Zhiqiang. Pulsed insert gas metral arc welding with feedback control[J]. Schweissen and Schneiden, 1985, 37(4): 54—55.

[2] Moore K L, Naidu D S, Ozcelik S. Moeling, sensing and control of gas metal arc welding [M]. Oxford: Oxford Elsevier, 2003.

[3] Yender R, Tyler J, Moore K L, *et al*. Gas metal arc welding control: Part 1—modeling and analysis[C] //In Nonlinear Analysis, Methods and Applications. Britain, 1997: 3101—3111.

[4] Lesnewich A. Control of melting rate and metal transfer in gas shielded metal arc welding, part I[J]. Welding Research Supplement, 1958, 37(8): 343—353.

[5] 胡跃明. 非线性控制系统理论与应用(第二版)[M]. 北京: 国防工业出版社, 2005.

[6] 王丰尧. 滑模变结构控制[M]. 北京: 机械工业出版社, 1995.

[7] Hassan K Khalil. 非线性系统(第三版)[M]. 北京: 电子工业出版社, 2005.

作者简介: 高忠林, 男, 1978 年出生, 博士研究生。研究方向为焊接过程先进控制方法的应用及焊接设备的开发。发表论文 2 篇。

Email: gaozhonglin@tju.edu.cn

[上接第 52 页]

5 结 论

(1) 高温合金等离子熔积成形的裂纹为热裂纹, 方向大多垂至于焊枪移动方向。

(2) 水冷跳跃路径成形条件下, 零件的温度场更均匀, 温度梯度和冷却速度显著降低; 成形中应力峰值降低近 12.5%, 维持在0.77 $R_{m(60\ ℃)}$左右, 成形后为0.85 $R_{m(25\ ℃)}$, 热裂倾向降低, 成形性较好。

参考文献:

[1] 宋建丽, 邓琦林, 葛志军, 等. 镍基合金激光快速成形裂纹控制技术[J]. 上海交通大学学报, 2006, 40(3): 548—552.

[2] 杨 健, 黄卫东, 陈 静, 等. 激光快速成形金属零件的残余应力[J]. 应用激光, 2004, 24(1): 5—8.

[3] 王桂兰, 吴圣川, 张海鸥. 复杂零件等离子熔积无模成形的温度场模拟[J]. 焊接学报, 2007, 28(5): 49—52.

[4] 刘 庄, 吴肇基, 吴景之, 等. 热处理过程的数值模拟[M]. 北京: 科技出版社, 1996.

[5] 董克权, 刘超英, 肖奇军. 双丝焊温度场仿真的热源模型研究[J]. 热加工工艺(焊接版), 2006, 35(3): 49—52.

作者简介: 吴圣川, 男, 1979 年出生, 博士研究生。研究方向为高性能金属零件无模制造中温度场和应力场的无网格及有限元快速模拟仿真。发表论文 9 篇。

Email: wushengchuan@gmail.com

Microstructures and formation of EBW joint of aluminum alloy LF2 to steel Q235 with transition metal Cu ZHANG Binggang, HE Jingshan, ZENG Ruchuan, FENG Jicai (State Key Laboratory of Advanced Welding Production Technology, Harbin Institute of Technology, Harbin 150001, China). p37—40

Abstract: Butt welding of dissimilar metal between Al alloy LF2 and carbon steel Q235 with the middle transition metal of Cu was carried out by electron beam welding. The microstructures, elements distribution in the joint were investigated by means of optical micrography, SEM and EDX. The result showed that the macrostructure in the joint can be divided into three zone. One is Fe based solid solution with a small amount of intermetallic compounds at the weld zone near to steel side. One is Al based solid solution with a definite store of Fe—Al and Al—Cu intermetallic compounds at the weld zone near to aluminium alloy. The other is mixed intermetallic compounds zone which consists of the several kinds of Fe—Al and Al—Cu intermetallic compounds at the middle weld, and its distribution is layered and banded. The analysis indicated that more intermetallic compounds were made in the weld although the transition metal Cu was used, particularly the multiple bedded and zonal intermetallic compounds formed and distributed in the middle weld are the main factor to influence the strength of the joint. Based on the analysis on microstructure of the joint, the physical model was founded to describe the forming process of dissimilar metal joint between Al alloy LF2 and carbon steel Q235 with transition metal Cu by EWB.

Key words: dissimilar metals; electron beam welding; microstructures of joint

Effects of activating fluxes on AC A-TIG weld penetration of magnesium alloy HUANG Yong, FAN Ding, YANG Peng, LIN Tao (State Key Laboratory of Gansu Advanced Non-ferrous Metal Materials, Lanzhou University of Technology, Lanzhou 730050, China). p41—44

Abstract: AC A-TIG welding experiments of magnesium alloy were carried out to study the effects of surface activating fluxes on weld penetration. Elements including Te, Ti and Si, oxides including SiO_2, TiO_2 and V_2O_5, halides including $MnCl_2$, $CdCl_2$ and ZnF_2 were used as activating fluxes, respectively. It is found that, Te powder, ZnF_2 and $CdCl_2$ all can increase weld penetration dramatically. Especially for Te powder, weld penetration reaches 1.6 times of that of conventional TIG welding. Weld depth width ratio reaches 0.43. Ti powder has little effect on weld penetration and weld width. All V_2O_5, SiO_2, TiO_2, $MnCl_2$ and Si powder decease weld penetration and weld width. Among the three activating fluxes improving weld penetration obviously, both Te powder and ZnF_2 refine weld grain. $CdCl_2$ coarsens weld grain a little. The results indicate that, electron adsorption with activating flux particles of Te powder, ZnF_2 and $CdCl_2$ can constrict arc and increase weld penetration of AC TIG welding of magnesium alloy.

Key words: magnesium alloy; alternating current activating tungsten inert-gas welding; activating flux; weld penetration

Microstructure and properties near interface zone of diffusion-bonded joint for Mg/Al dissimilar materials LIU Peng[1], LI Yajiang[2,3], WANG Juan[2] (1. Key Laboratory for Advanced Materials Processing Technology, Ministry of Education, Tsinghua University, Beijing 100084, China; 2. Key Laboratory of Liquid Structure and Heredity of Materials, Ministry of Education, Shandong University, Jinan 250061, China; 3. State Key Laboratory of Advanced Welding Production Technology, Harbin Institute of Technology, Harbin 150001, China). p45—48

Abstract: The interface zone of Mg/Al diffusion-bonded joint is constituted with Al transition layer (Mg_2Al_3 phase), middle diffusion layer (MgAl phase) and Mg transition layer (Mg_3Al_2 phase). Some diffusion holes exist between the Al transition layer and middle diffusion layer observed by SEM. It is unfavorable to obtain diffusion-bonded joint of good performance. With the increase of heating temperature, the shear strength of joint interface shows the trend of increasing firstly and then decreasing. The highest shear strength is about 18.94 MPa when the heating temperature is 475 ℃, holding time is 60 min and pressure is 0.081 MPa. The microhardness test indicated that the microhardness of diffusion zone is about 260—350 HM. However, and the diffusion zone exist three different hardness regions. With the increase of heating temperature, the microhardness and diffusion width of interface diffusion zone increase gradually.

Key words: Mg/Al dissimilar materials; vacuum diffusion bonding; microstructure; shear strength

Plasma deposition dieless manufacturing of turbine parts: thermal stress control and process optimization Wu Shengchuan[1], ZHANG Hai'ou[1], WANG Guilan[2], XIONG Xinhong[2] (1. State Key Laboratory of Digital Manufacturing Equipment and Technology, Huazhong University of Science and Technology, Wuhan 430074, China; 2. State Key Laboratory of Material Processing and Die & Mould Technology, Huazhong University of Science and Technology, Wuhan 430074, China). p49—52, 56

Abstract: Plasma deposition dieless manufacturing (PDM) is a rapid heating and solidification process, in which how to avoid cracks and distortions is a key problem. Therefore, a full understanding on the evolution of temperature field variables is essential to achieve a steady state and robust PDM process. To explore the thermal behaviors of this process, the preheated and water-cooled programs for the fabrication of superalloy turbine parts have been designed respectively. Their temperature fields are then evaluated numerically by finite element method. Analysis results show that the water-cooled scheme exhibits lower hot crackability and better formability, which coincides well with experimental results. The stress distributions are further analyzed with the optimized scanning path based on the water-cooled scheme above. Computational results indicate that reasonable process-cooled conditions can reduce peak stresses and the temperature and stress gradients, and also demonstrate the feasibility and validity of this approach. More importantly, the water-cooled scheme can be easily implemented and remarkably improves the possibly-intended formability of the PDM.

Key words: plasma deposition dieless manufacturing; high energy density beam; stress distribution; finite element method; hot crackability

Simulation of feedback linearization and sliding mode control in

GMAW systems GAO Zhonglin[1], HU Shengsun[1], YIN Fengliang[1], WANG Rui[2] (1. College of Material Science and Engineering, Tianjin University, Tianjin 300072, China; 2. College of Electrical and Automation, Hebei Technology University, Tianjin 300130, China). p53—56

Abstract: An investigation was made to the gas metal arc welding (GMAW) systems, and further for the control purpose a dynamic system and control model was proposed according to the characteristics of the GMAW systems. By means of the feedback linearization procedure of differential geometry, an equivalent, fully controllable and linear model was derived via a homomorphic transformation and a sliding mode controller was constructed for the GMAW system. The simulation results by Matlab showed the effectiveness of the proposed controller and the method is satisfied with exact control of welding arc length.

Key words: gas metal arc welding; sliding mode control; feedback linearization; robust

Effects of beneficial inclusions in CGHAZ of oxides metallurgy steel LI Zhanjie[1], YU Shengfu[1], LEI Yi[2], YAO Fang[1] (1. School of Materials Science and Engineering, Huazhong University of Science and Technology, Wuhan 430074, China; 2. School of Mechanical and Electronic Engineering, China University of Petroleum, Dongying 256001, Shangdong, China). p57—60

Abstract: Using physical simulation method, influence of beneficial inclusions on microstructure was studied in coarse grain welding heat affected zone (CGHAZ) of the oxides metallurgy steel. The inclusions which induced nucleation of acicular ferrite were observed by transmission electron microscope and the chemical composition was also analyzed by energy dispersive X-ray spectroscopy. Results indicated that the beneficial inclusions in CGHAZ of the prepared steel are oxide complexes composed of MnO, TiO_x, SiO_2 and Al_2O_3 or oxide-sulfide complexes composed of such oxides and MnS, CuS or (Mn, Cu)S, and their diameter is 0.2—0.6 μm. During welding process, beneficial inclusions can induce multidimensional nucleation of acicular ferrite and sympathetic nucleation as well, which make the acicular ferrite in CGHAZ interlocked and grains refined apparently. The microstructure in CGHAZ of the prepared steel has the ability of self-refining.

Key words: oxides metallurgy; beneficial inclusion; acicular ferrite

Dada acquisition and defects analysis in resistance spot welding process based on parallel port NIU Yong[1], XUE Haitao[2], ZENG Zhoumo[1], LI Yongyan[2] (1. State key Laboratory of Precision Measuring Technology and Instrument, Tianjin University, Tianjin 300072, China; 2. School of Material Science and Engineering, Hebei University of Technology, Tianjin 300132, China). p61—64, 80

Abstract: An efficient data acquisition system was built to collect welding parameter of aluminum alloys shock wave resistance spot welding by using single chip processor and process computer. The communication port of the system between single chip processor and process computer is parallel port. This system have many advantages such as better anti-jamming performance, high reliability, better expansion capacity, fast picking rate and transfer rate. The software of this system developed by LabVIEW has functions such as communication, data manipulation, the database and the data analysis function. A systematic analysis based on acquisition data shows that the earlier splash can be identified by "collapsing abrupt change" of tip voltage signal and "high frequency restlessness abrupt change" of electrode force signal, but for later splash, it can be identified only by "high frequency restlessness abrupt change" of electrode force signal. Moreover the incomplete fusion can be identified by "thermal expansion rise value" and "forging force drop value" extracting from electrode displacement.

Key words: aluminum alloy resistance spot welding; data acquisition; data analysis; welding defect

Finite element analysis on soldered joint reliability of QFP device with different lead materials ZHANG Liang, XUE Songbai, LU Fangyan, HAN Zongjie* (College of Materials Science and Technology, Nanjing University of Aeronautics and Astronautics, Nanjing 210016, China). p65—68

Abstract: Finite element method was used to simulate the residual stress in soldered joints of QFP device with three kinds of lead materials. The results indicate that all the stress concentration area in soldered joint is at the sharp corner of interior part of the joint where is the weakest area of the joint. Comparing with the simulating results about alloy-42, copper alloy and Kovar alloy, especially analyzing the nephograms of equivalent strain and the strain and stress curves, it is shown that the stress and strain makes periodic change with the time, simultaneously has the accumulated tendency, and the value of strain and stress in the soldered joint of alloy-42 gull is the least, and the value is middle in the joint of Kovar alloy, and the value was largest in the joint of copper alloy. The simulating results may provide a theory guide for developing novel lead material as well as selecting lead materials in production.

Key words: finite element method; residual stress; strain and stress; lead material

Bonding interface of containing-Ti prealloy based CuMn and diamond grit via brazing YUAN Jie, ZHAO Ning, NAN Junma, XU Kewei* (State Key Laboratory of Mechanical Behavior for Materials, Xi'an Jiaotong University, Xi'an 710049, China). p69—72

Abstract: A containing-Ti prealloyed powder was designed to be used as an adhesion matrix to increase the diamond retention, and then made from the Cu and Mn by gas atomization. An analysis was made to the metal-diamond bonding interface after the bulk composites being hot-pressed in rough vacuum brazing, which is produced according to the characteristics of the containing-Ti powder with the melting temperature (about 1 151 K) determined by thermal analyzer, and the liquidity and spreadability were observed experimentally. It was found that the discrete island-shaped TiC occurs on the diamond surface, and the contents of Ti and C change obviously in both sides of the interface with Ti rich in the region closed to the diamond and C rich in the region closed to a matrix, because of the chemical reaction based on the introduction of a strong carbide-forming element Ti to the prealloyed powders.

Key words: brazing; bonding interface; containing-Ti preal-